JOURNAL OF CATALYSIS **178,** 328–337 (1998)
ARTICLE NO. CA982171

Catalytic Cracking of Vacuum Gas Oil on the Dealuminated Mordenites

Kyong-Hwan Lee,*,[1] Youn-Woo Lee,† and Baik-Hyon Ha*

*School of Chemical Engineering, College of Engineering, Hanyang University, 17 Haengdangdong, Sungdongku, Seoul 133-791, Korea; and †Division of Environment and CFC Technology, Korea Institute of Science and Technology, 39-1 Haweolkok-dong, Sungbuk-ku, 136–791, Korea

Received August 21, 1997; revised February 25, 1998; accepted May 26, 1998

Catalytic cracking of vacuum gas oil was carried out at 500°C over two series of mordenites treated by either steam/HCl or HF. Secondary mesopores were formed in the mordenite by these treatments and their volumes increased with the degree of dealumination, whereas the micropore volumes decreased proportionately. The conversion of gas oil and the yield of gasoline and kerosene + diesel were correlated with the acid-amount/mesopore-volume ratio. A maximum conversion and yield were observed at a point of acid-amount/mesopore-volume ratio. This maximum point was interpreted as an optimum condition for the cracking activity between two inverse tendencies. The one is the decreasing tendency of cracking activity with reducing acid density. The other is the one increasing in activity with an increasing volume of the mesopore with silica/alumina ratio for both conversion of VGO and yields of gasoline and kerosene + diesel. On the treated mordenite of higher silica/alumina ratio, more olefins were formed due to a low rate of hydrogen transfer reaction. Aromatics are found to be formed via cyclization of olefins which can occur inside an enlarged mesopore of dealuminated mordenite. The largest content as an alkyl-aromatic compound in the produced gasoline was toluene, which was possibly interpreted as the diffusion limitation in the formation of higher alkyl-branched aromatics.

INTRODUCTION

Catalytic cracking of vacuum gas oil on various zeolites has been carried out to investigate their activity, selectivity, and deactivation properties (1–4). Extensive research into the fundamental aspects of catalytic cracking of numerous pure hydrocarbons such as *n*-octane, cumene, 1-phenylheptane, *n*-heptane, *n*-decane, *n*-dodecane, *n*-tetradecane, and *n*-alkanes (C_7-C_{14}) have also been undertaken over different type zeolites (5–10, 13). The zeolites used as cracking catalysts differ widely in their channel structures, pore diameters, and, also, in their Si/Al ratios. Among these properties, the aluminum density in the zeolite is the main factor controlling pore volume, stability, and hydrogen transfer reaction during cracking of the hydrocarbon (12). Corma *et al.* have demonstrated that the catalytic cracking of hydrocarbons over zeolites with different Si/Al ratios shows obviously different product distributions dependent on the the hydrogen transfer rate of bimolecular reactions which require the presence of two close acid sites (13).

Dealumination of the zeolite by various pretreatments, such as steaming and acid-extraction, lead to the formation of secondary mesopores within the channels of the zeolite (14–16). The hysteresis phenomena in their isotherm plots were observed from the adsorption/desorption isotherms of nitrogen (17). The magnitude of the hysteresis increases with successive treatments of steam/HCl, which implies increasing mesopore volume with the increasing Si/Al ratio (18). The introduction of mesopores in mordenite could provide the accessibility of a large amount of molecular reactant into the active site.

The present investigation is designed to gain further information on the effects of dealumination of mordenite on the activity and selectivity of the catalytic cracking of vacuum gas oil, especially on the roles of two parameters: the acidity reduction and the increase of secondary mesopore volume through the dealumination process by steam/HCl- and HF-treatments.

EXPERIMENTAL

Vaccum Gas Oil

The average molecular weight of the vacuum gas oil (VGO) used in this study as a reactant ranged from 360 to 380 (27). The average composition ranged between 10–15 vol% for paraffin, 40–50 vol% for naphthene, and 35–50 vol% for aromatic.

Preparation of Catalysts

Starting with Na-type mordenite, NaM (granule type of Norton Zeolon 900) was ion-exchanged with 1 *N* ammonium chloride solution at 80°C to prepare NH_4M. The

[1] Corresponding author. E-mail: Baikhha@email.hanyang.ac.kr. Present address: Environment Remediation Research Center, Korea Institute of Science and Technology, 39-1 Haweolkok-dong, Sungbuk-ku, Seoul, 136–791, Korea.

0021-9517/98 $25.00

NH_4M was washed with distilled water, dried at 120°C overnight and calcined at 500°C for 5 h to convert to HM. HM was treated with 100% steam for 3 h and then calcined at 500°C for the same period. Steamed HM was denoted as $SM_{6.5}$, in which 6.5 is the weight ratio of SiO_2/Al_2O_3. In order to construct the secondary mesopores in the mordenite, the HM was treated with 6 *N* HCl at 90°C for 4 h, 6 h, or 21 h and then steamed at 500°C for 3 h, 6 h, or 10 h. Such steamed mordenites were treated with 0.01 *N* HCl at 90°C for 2 h to remove separated aluminum oxide species from the framework in the pore channel. These samples were classified as $SM_{15.5}$, SM_{20}, or SM_{39}, respectively, in which subscripts indicate the SiO_2/Al_2O_3 ratios.

$SM_{6.5}$ was dealuminated by treating it with 0.5 *N* HF solution at room temperature for 192 h, 240 h, 384 h, or 528 h to prepare FM series catalysts. These samples were classified as FM_{17}, $FM_{17.5}$, FM_{21}, and $FM_{21.5}$, respectively. Each dealuminated mordenite was finally treated with steam at 500°C for 3 h to remove HCl or HF bonded weakly on a surface of mordenite and then calcined at 500°C for 3 h.

Characterization of Catalysts

For chemical analysis, the sample was mixed with dilithium tetraborate as flux, fused at 1000–1200°C, dissolved in water, and measured by X-ray fluorescence (Philip, PW-1480).

All samples were pretreated in vacuum at 300°C for 6 h for the nitrogen adsorption. The adsorption/desorption isotherms of nitrogen on the modified mordenites were obtained at liquid nitrogen temperature using Micromeritics ASAP-2000. From the isotherm, specific surface area of BET, average pore diameter and the pore volume were determined. The distinction between micropore and mesopore was made by the T-plot method (19). The pore size distributions were obtained from nitrogen desorption branches using the BJH method.

For the infrared spectra, the sample was pressed into thin wafers (9 mg/cm^2) and out-gassed overnight at 400°C in vacuum (3×10^{-3} Torr.). The spectra of hydroxyl group were measured in the range of 4000–3000 cm^{-1} at room temperature by using the Magma-IR spectrometer (Nicolet Co.). For the Brönsted and Lewis acid, the pyridine was admitted into the IR cell at room temperature and the samples were equilibrated at 150°C, 250°C, and 350°C for 1 h in a vacuum (3×10^{-3} Torr.) prior to measuring the spectra in the region of 2000–1300 cm^{-1}.

The coke formed during the cracking reaction was analyzed by an elemental analyzer (Heraeus Co., vario EL). The evolved gas, such as carbon dioxide, sulfide dioxide, and water from the coke of the catalyst was analyzed by GC with TCD.

Reaction Procedure and Analysis

The catalytic activity was measured in a modified microactivity tester (MAT), based on ASTM D-3907-87 (18). A catalyst of 1.7 g was loaded in the micro-reactor and pretreated with nitrogen gas for 30 min at 500°C. The VGO (0.9 ml) was injected into the reactor with a contact time of 75 s and a catalyst-to-oil ratio (g-catalyst/g-oil) of 2. During the reaction, the liquid product was collected in an ice-cooled reservoir. The gaseous product was trapped by water displacement. At the end of the run, the reactor was purged with nitrogen for 20 min. The purged gas was also collected for analysis. The trapped liquid products were analyzed by gas chromatography (Shimadzu, GC-14A) with a capillary column (CBP-1, 25 m X 0.25 μm) and FID detector. A chromatogram of the gasoline was identified with a mass spectrum analyzer (Shimadzu, GCMS-QP5000). The hydrocarbons in the gasoline were classified as paraffin, olefin, naphthene, and aromatic. The gasoline and kerosene + diesel (K + D) were fractionated by HT-SIMDIST (Fisons) with a capillary column (7 m × 0.58 mm) coated with metal silicon.

RESULTS AND DISCUSSION

Characterization

The characteristics of the modified mordenites used in this study are presented in Table 1. The weight ratio of SiO_2 to Al_2O_3 over the mordenite treated by steam/HCl increased up to 39, but the HF-treatment increased up to 21.5 at most. The steam/HCl treatment eliminates only aluminum atoms from the framework, but HF could simultaneously remove aluminum as well as silicon (21), which limited the increase of the SiO_2/Al_2O_3 ratio. The slight decrease in the surface area of the HF-treated mordenite at the higher silica/alumina ratio may be explained by the partial collapse of the structure, due to the simultaneous removal of aluminum and silicon.

The mesopore volume in Table 1 was obtained by extraction of the micropore volume from the total volume. $SM_{6.5}$ was the starting solid for the HF- and steam/HCl-treatments $SM_{6.5}$ has an 86% micropore volume to the total, which is the same as that of HM. However, $SM_{15.5}$ has a sharply increased mesopore volume, which indicates a transformation mostly of micropore to mesopore in this step of the treatment. At more than 15.5 of SiO_2/Al_2O_3 ratio, both micropore and mesopore show little or gradual increase in steam/HCl-treated mordenite. For the HF-treated mordenites, FM_{17} also has a sharply increased mesopore volume. The mesopore volume of more than 17 of SiO_2/Al_2O_3 ratio gradually increased with the SiO_2/Al_2O_3 ratio by the simultaneous removal of silicon as well as aluminum, whereas the micropore volume remained practically constant.

TABLE 1

Characterized Data for Mordenites Treated by either Steam/HCl(a) or HF(b)

Catalyst(a)	HM	$SM_{6.5}$	$SM_{15.5}$	SM_{20}	SM_{39}
SiO_2/Al_2O_3 (wt. ratio)	5.9	6.5	15.5	20	39
Na_2O(wt.%)	0.40	0.33	0.03	—	—
BET surface area(m^2/g)	457	500	542	533	534
Total pore volume(cc/g)	0.2271	0.2170	0.2793	0.2942	0.3101
Micropore volume(cc/g)	0.1946	0.1858	0.1686	0.1736	0.1763
Mesopore volume(cc/g)	0.0325	0.0312	0.1107	0.1206	0.1338
Catalyst(b)	$SM_{6.5}$	FM_{17}	$FM_{17.5}$	FM_{21}	$FM_{21.5}$
SiO_2/Al_2O_3 (wt. ratio)	6.5	17	17.5	21	21.5
Na_2O(wt. %)	0.33	1.2	1.7	0.08	0.03
[a]F (surface atomic %)	—		1.2	1.3	1.2
BET surface area(m^2/g)	500	527	533	499	480
Total pore volume(cc/g)	0.2170	0.2806	0.2939	0.2828	0.2925
Micropore volume(cc/g)	0.1858	0.1772	0.1811	0.1698	0.1637
Mesopore volume(cc/g)	0.0312	0.1034	0.1128	0.1130	0.1288

[a] XPS analysis.

The pore size distributions of both series of the samples are shown in Fig. 1. All samples show a unique peak centered at 3.8 nm mesopore diameter created during hydrothermal and chemical treatment (18). The peak volume (at 3.8 nm) of the mesopore in steam/HCl-treated mordenites increased with the gradual dealumination process. On the other hand, that of HF-treated mordenite increased sharply up to 17.5 of SiO_2/Al_2O_3 ratio and then slightly decreased, enlarging the volume at the lower diameter region rather than at the peak diameter.

The Brönsted (1540 cm^{-1}) and Lewis (1450 cm^{-1}) acid sites were determined by IR spectroscopy of adsorbed pyridine at 150°C and 350°C over the two series of the treated mordenites. The spectra are shown in Fig. 2. The peak height (arbitrary unit) of 1540 (B) and 1450 cm^{-1} (L) and total acid amount (B- + L-acid), the ratio of L/B, and the relative ratio of the peak at 150°C to that at 350°C as a parameter of acid strength are presented in Table 2. In the case of steam/HCl-treated mordenites, the amount of Brönsted acid decreased rapidly at 15.5 of the SiO_2/Al_2O_3 ratio and remained almost constant as the SiO_2/Al_2O_3 ratio increased from 15.5 to 39. This result agrees with the IR-spectra of OH group presented in Fig. 3A. The 3610 cm^{-1} band associated with the framework aluminum of the Brönsted site (20) also decreased also sharply at 15.5 of the SiO_2/Al_2O_3 ratio and then kept constant above 15.5. The newly formed 3740 cm^{-1} band of the silanol group at the removed aluminum site of the framework increased with the SiO_2/Al_2O_3 ratio through the dealumination.

The Brönsted and Lewis acid amounts of HF-treated mordenites decreased with the SiO_2/Al_2O_3 ratio. However, FM_{17} revealed pronounced Lewis acid (150°C), probably from the new formation of the Lewis site resulting from the replacement of the hydroxyl group of extra-aluminum oxide and/or of the framework aluminum with F during HF-treatment (21, 22).

The L/B at 150°C for the two series of samples with SiO_2/Al_2O_3 is also presented in Table 2. Steam/HCl-treated mordenites have a higher ratio of L/B than HF-treated mordenites at the same level of the SiO_2/Al_2O_3 ratio. However, the ratios of L/B above 15 of SiO_2/Al_2O_3 were almost constant despite the increase in the SiO_2/Al_2O_3 ratio.

As an indicator of acid strength, the spectra height ratio of the spectrum of adsorbed pyridine was obtained at 350°C and 150°C. The ratios of B(350°C)/B(150°C) and L(350°C)/L(150°C) decreased as the SiO_2/Al_2O_3 ratio

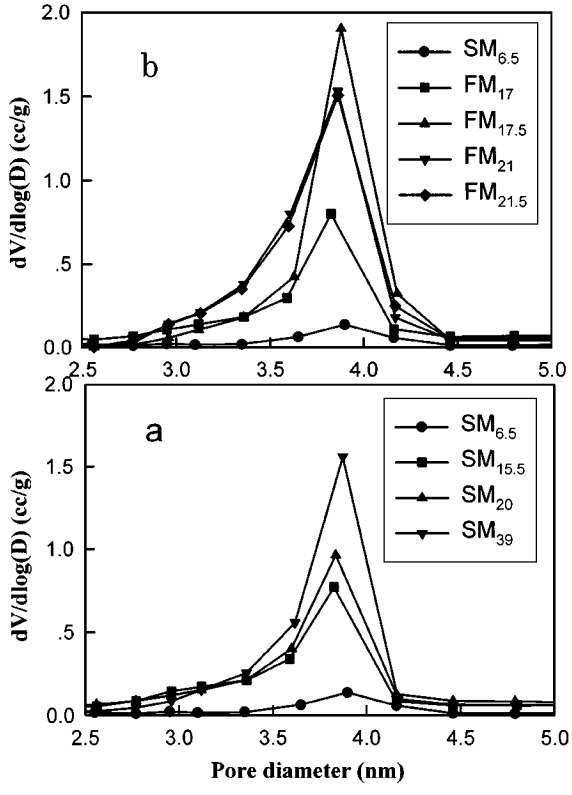

FIG. 1. Pore size distributions obtained by nitrogen desorption isotherm branches over mordenites treated by either steam/HCl (a) or HF (b).

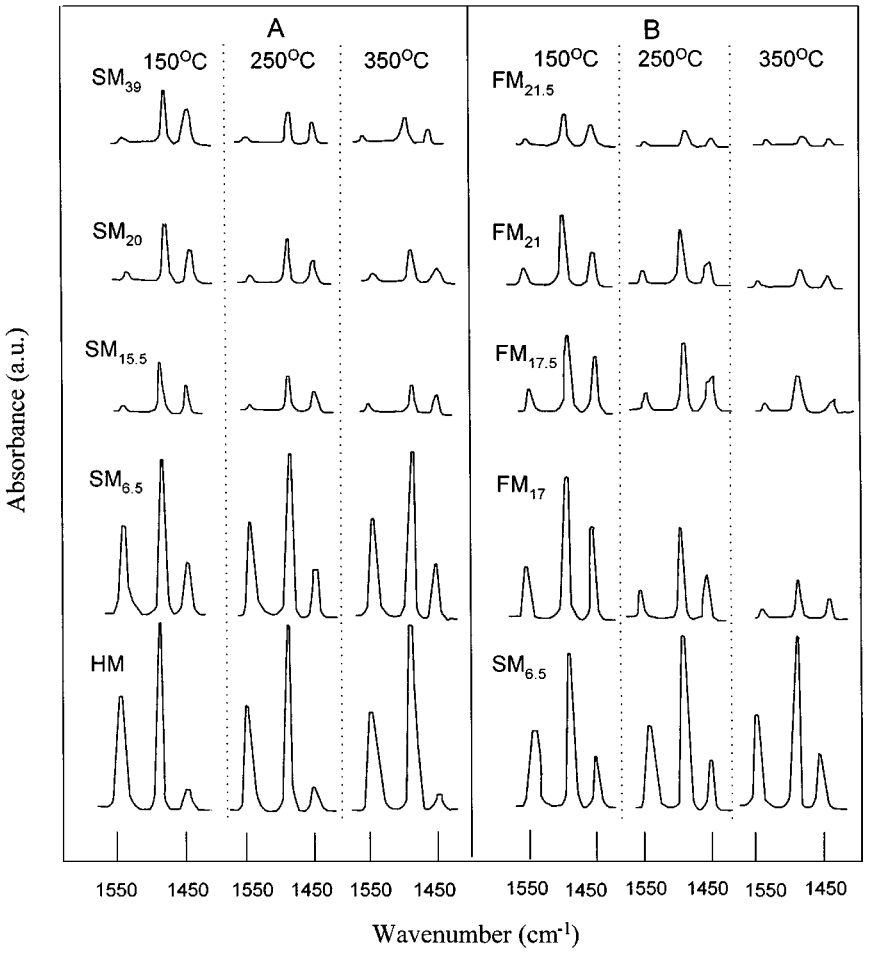

FIG. 2. IR spectra after pyridine adsorption on mordenites treated by either steam/HCl(A) or HF(B) at room temperature followed by desorption at various temperatures.

increased for both series of samples. The acid strength of the steam/HCl-treated mordenites was higher than that of the HF-treated mordenites at the same level of the SiO_2/Al_2O_3 ratio.

Activity

As a measure of the cracking activity of VGO over the mordenites, the conversion of VGO, gasoline yield, and

TABLE 2

The Intensity of IR Spectra of Brönsted Acid Site (1545 cm^{-1}) and Lewis Acid Site (1450 cm^{-1}), Total Acid Amount (B + L), L/B, and Acid Strength Determined as the Arbitrary Unit by Pyridine Adsorption for Treated Samples (20)

	Brönsted acid site		Lewis acid site		Total acid amount	Acid type ratio	Acid strength	
Sample	B (150°C)	B (350°C)	L (150°C)	L (350°C)	B + L (150°C)	L/B (150°C)	B(350°C)/ B(150°C)	L(350°C)/ L(150°C)
HM	12.9	10.5	3.1	2.3	16.0	0.24	0.81	0.74
$SM_{6.5}$	9.9	11.1	5.5	6.0	15.4	0.56	1.12	1.20
$SM_{15.5}$	1.3	1.0	4.0	2.3	5.3	3.08	0.77	0.58
SM_{20}	1.5	1.0	4.4	2.5	5.9	2.93	0.67	0.57
SM_{39}	1.5	1.0	4.7	1.7	6.2	3.13	0.67	0.36
FM_{17}	5.2	2.2	10.8	2.8	16.0	2.08	0.42	0.26
$FM_{17.5}$	3.4	1.4	6.8	1.4	10.2	2.00	0.41	0.21
FM_{21}	3.0	1.0	4.4	0.6	7.4	1.47	0.33	0.14
$FM_{21.5}$	1.4	0.6	3.4	0.4	4.8	2.43	0.42	0.12

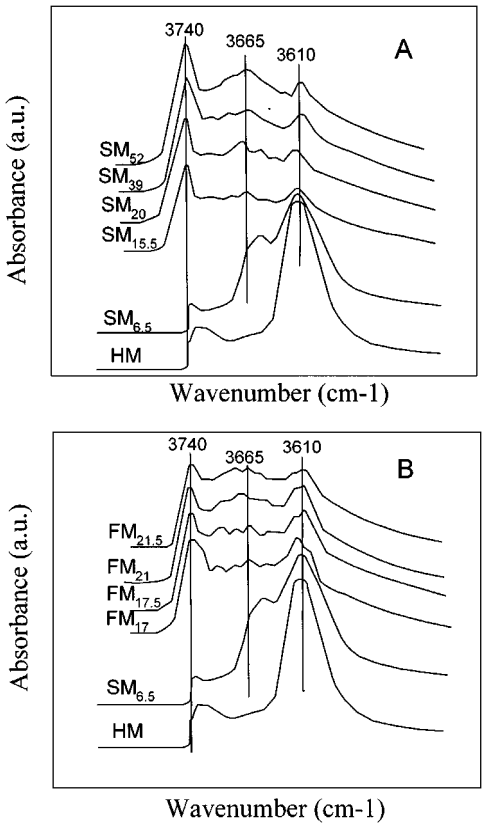

FIG. 3. IR spectra of OH band sites after calcination over mordenites treated by either steam/HCl(A) or HF(B).

kerosene + diesel yield were determined for two series of the samples. We supposed that the conversion of VGO and the yields of gasoline and kerosene + diesel could be controlled by two factors. The first is the number of acid sites of the catalysts which decrease with the SiO_2/Al_2O_3 ratio. The second is the pore size, especially mesopore size, which increases with the SiO_2/Al_2O_3 ratio and can provide improved accessibility and cracking activity of the VGO. In other words, the activity due to the number of acid sites is reduced with the SiO_2/Al_2O_3 ratio. However, the improved accessibility of the VGO into the mesopore may increase the reaction rate. A possible optimum point could be supposed between two tendencies. Therefore, we introduced a ratio of acid-amount (B + L)/mesopore-volume, in which acid-amount is the percentage of acid amount based on 16(a.u.) of HM and the unit of mesopore-volume formed at 3.8 nm diameter (Fig. 1) is used as the cubic centimeter per gram.

Three interesting plots were obtained for the conversion of the VGO, gasoline yield, and kerosene + diesel yield (K + D) against the acid-amount/mesopore-volume as shown in Fig. 4 and Fig. 5 for the two series of the samples. The catalysts of a large mesopore volume such as $FM_{21.5}$, FM_{21}, and SM_{39} show low conversion of the VGO due to the low acid amount, whereas the catalyst with a high acid amount, such as $SM_{6.5}$ and FM_{17}, shows low cracking activity due to a low mesopore volume. The higher range of this maximum point means a small quantity of mesopores

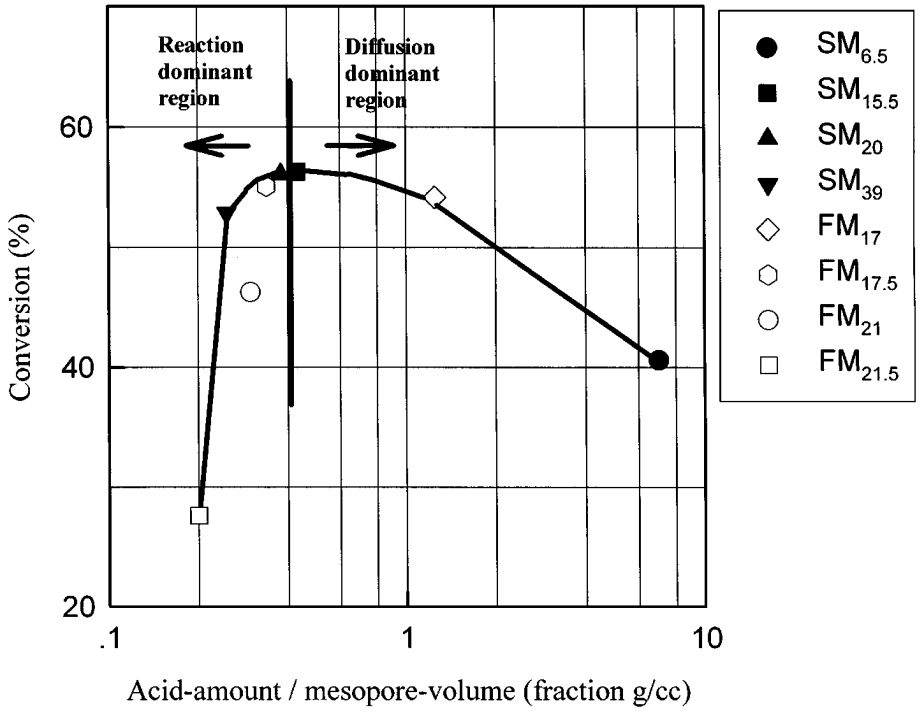

FIG. 4. Conversion obtained from cracking of vacuum gas oil as a function of acid-amount/mesopore-volume over mordenites treated by either steam/HCl or HF: reaction temperature, 500°C; WHSV, 24 h^{-1}.

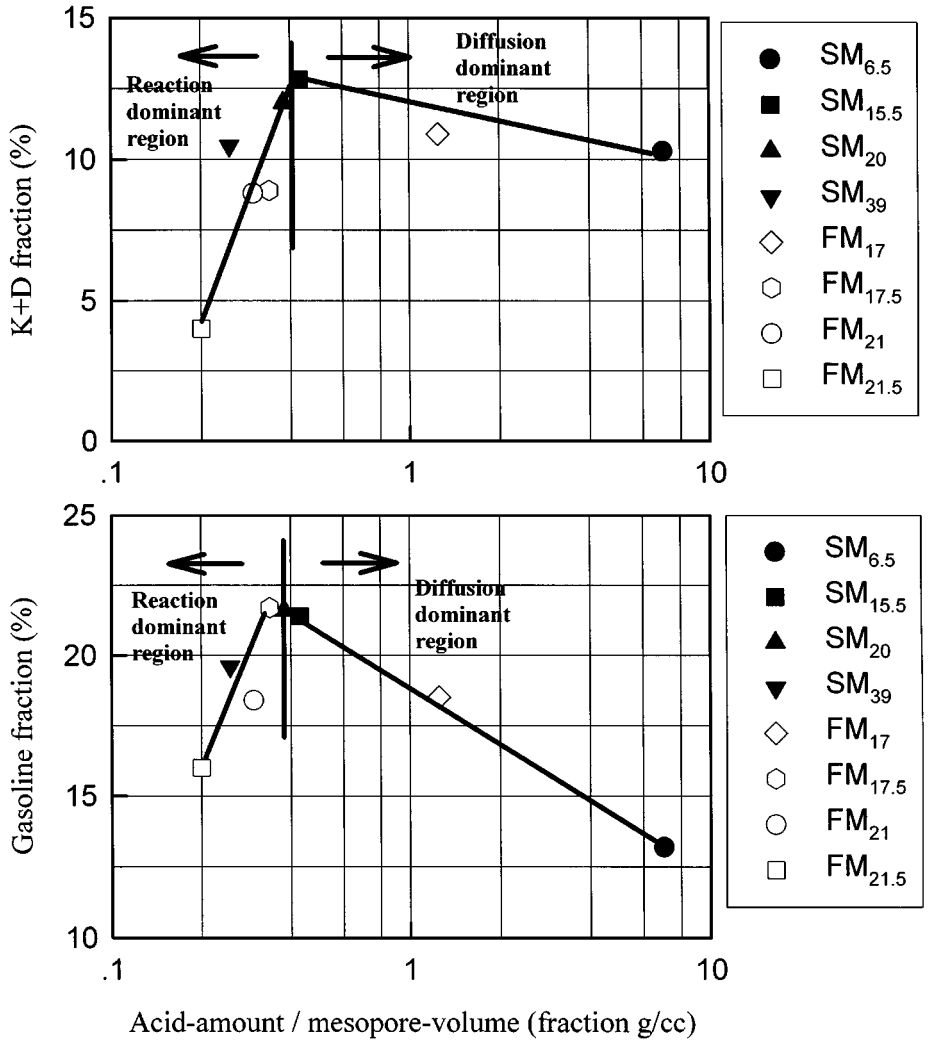

FIG. 5. Fraction of gasoline and kerosene + diesel in liquid product obtained from the cracking of vacuum gas oil as a function of acid-amount/mesopore-volume over treated mordenites.

and large amounts of acid site, and in this region, VGO hardly diffuses toward the active site of the inside pores. Diffusion limitation plays a crucial role in the cracking of VGO. The lower range indicates a large quantity of mesopore volume and small amounts of acid sites. In this region, the acid amount plays a leading role in the cracking of VGO. In all treated mordenites, the liquid produced has a greater gasoline fraction than K + D fraction as shown in Fig. 5. This means that the pore structure of mordenites mainly produces gasoline components with carbon number of below 11. At the diffusion-dominant region in Fig. 5, the gasoline fraction is sharply decreased with the acid-amount/mesopore-volume ratio than with the K + D fraction. It could be considered that the K + D is mainly produced on the external and macro surface of the treated mordenite, while the gasoline product is shape sensitive and produced within the mesopore.

Coke on the catalysts, determined by elemental analysis, is also presented as a function of the acid-amount/mesopore-volume in Fig. 6. The coke amount increases rapidly at a lower acid-amount/mesopore-volume ratio. It suggests that both increase of the acid amount and of the micropores may increase the coke formation. Therefore, $FM_{21.5}$ shows the lowest content of coke. $SM_{6.5}$ deposited more coke, compared to the dealuminated mordenite, because the coke could be easily retained in the micropores of $SM_{6.5}$ as polymerized large molecules (24). Also $SM_{6.5}$ has a high acid site density, compared to the dealuminated mordenites and produces more coke content by means of high intermolecular hydrogen transfer reactions between adsorbed alkyl-aromatic species (24). Although $SM_{15.5}$ and SM_{20} treated by steam/HCl and FM_{17} treated by HF had almost a similar conversion, the coke amount in FM_{17} increased by a factor of 1.5, compared to $SM_{15.5}$ and SM_{20}.

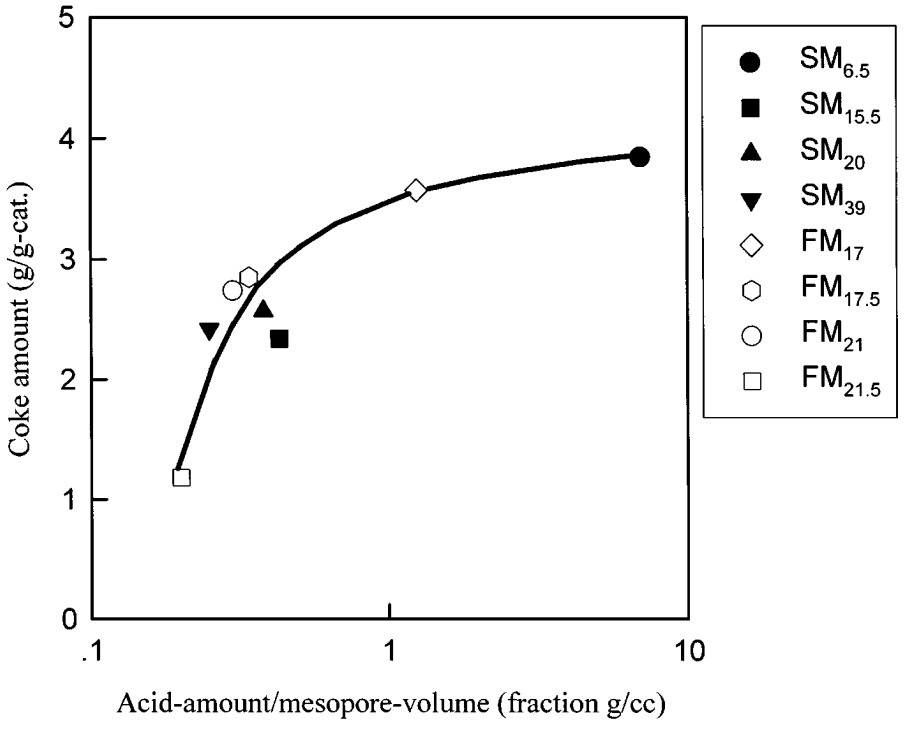

FIG. 6. Coke amount formed during cracking of vacuum gas oil over mordenites treated by either steam/HCl or HF.

It can be explained that FM_{17} had more Lewis sites, which produce more coke (5) than $SM_{15.5}$ and SM_{20} as shown in Table 2.

Product Distribution

The product distributions from cracked VGO on two series of mordenites were shown in Table 3. VGO has paraffins, naphthenes, and heavy aromatics as major components (25). The product has lower olefins and light aromatics of about 80% in gasoline fraction, although the VGO stock is mainly comprised of naphthenes and aromatics with 1-, 2-, and 3-ring alkylated species (25). The *iso*-olefins are formed through cracking, a ring opening and an isomerization of heavy aromatics and/or naphthenes in the feed stock. Therefore, light mono-aromatics are possibly formed by cyclization of the *iso*-olefin.

The olefins in Table 3 comprise mainly the C_5 and C_6 components, whereas aromatics comprise the C_7 and C_8 components. This implies that the olefins of C_7 and C_8 are directly transformed into mono-aromatics such as toluene, xylene, and ethylbenzene by means of cyclization. The lower the fraction of paraffin produced compared to that of the olefin means there is a low hydrogen transfer rate on the mordenites which have a low acid site density (26).

In the steam/HCl-treated mordenite the olefin content decreased, whereas the aromatics increased with the SiO_2/Al_2O_3 ratio. However, the olefin fraction in the product over HF-treated mordenites indicates no clear

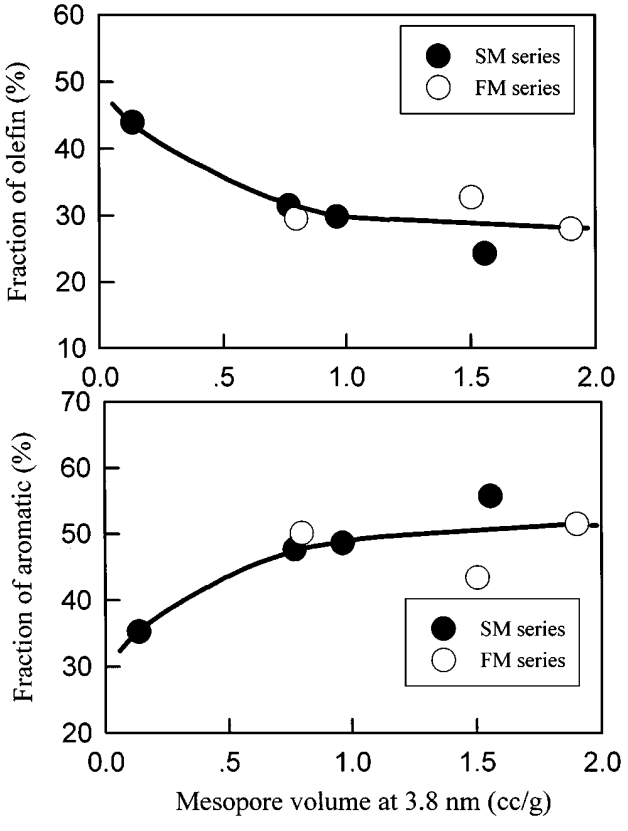

FIG. 7. Fraction of olefin and aromatic in gasoline as a function of the mesopore volume over mordenites treated by either steam/HCl or HF.

TABLE 3

Hydrocarbon Distribution in the Gasoline Obtained from Cracking of Vacuum Gas Oil over Mordenites Treated by either Steam/HCl or HF

	$SM_{6.5}$	$SM_{15.5}$	SM_{20}	SM_{39}	FM_{17}	$FM_{17.5}$	FM_{21}	$FM_{21.5}$
Conversion	40.6	56.3	56.1	52.9	54.2	55.1	46.3	27.6
Paraffin	13.64	13.87	15.54	13.88	13.35	14.51	14.45	14.24
Olefin	43.99	31.49	29.85	24.29	29.56	28.02	34.79	32.73
Naphthene	7.12	6.99	5.98	6.09	6.96	5.93	7.57	9.61
Aromatic	35.25	47.66	48.63	55.74	50.12	51.54	43.19	43.42
Total(wt.%)	**100**	**100.01**	**100**	**100**	**99.99**	**100**	**100**	**100**
Paraffin (wt.%)	**13.64**	**13.87**	**15.54**	**13.88**	**13.35**	**14.51**	**14.45**	**14.24**
i-C5	4.99	4.22	5.71	4.33	4.23	4.84	4.33	5.25
i-C6	4.54	5.58	6.36	5.88	5.01	5.50	5.22	4.96
i-C7	2.71	2.60	2.57	2.50	2.39	2.73	2.83	2.14
i-C8	1.40	1.47	0..90	1.17	1.72	1.44	2.07	1.89
Olefin (wt.%)	**43.99**	**31.49**	**29.85**	**24.29**	**29.56**	**28.02**	**34.79**	**32.73**
n-C5	8.58	6.06	5.96	4.39	5.01	4.63	5.10	5.69
i-C5	9.85	5.88	7.15	4.70	5.21	5.32	5.82	6.90
i-C6	15.43	12.38	11.52	10.01	11.29	11.32	13.66	10.86
i-C7	6.27	4.17	3.09	3.12	5.01	4.02	6.15	6.20
i-C8	3.86	3.00	2.13	2.07	3.04	2.73	4.06	3.08
Naphthene (wt.%)	**7.12**	**6.99**	**5.98**	**6.09**	**6.96**	**5.93**	**7.57**	**9.61**
Methylcyclopentane	2.64	2.56	2.69	2.45	2.27	2.46	2.47	2.14
Methylcyclohexane	1.52	1.46	1.41	1.30	1.12	1.28	1.46	1.41
Dimethylcyclopentane	1.63	1.56	0.77	1.05	1.80	1.04	2.27	3.88
Methylcyclohexene	1.33	1.41	1.11	1.29	1.77	1.15	1.37	2.18
Aromatic (wt.%)	**35.25**	**47.66**	**48.63**	**55.74**	**50.12**	**51.54**	**43.19**	**43.42**
Benzene	5.42	6.08	5.95	6.69	7.37	6.66	6.57	5.87
Toluene	10.15	13.30	14.36	16.18	14.94	14.87	11.87	11.19
Ethylbenzene	3.13	4.04	4.01	4.42	3.78	3.74	3.52	3.37
M,P-xylene	4.47	6.95	7.59	9.21	7.50	8.15	5.66	6.00
O-xylene	2.26	3.52	3.28	4.26	3.69	4.31	3.27	3.32
Propylbenzene	1.16	1.53	1.39	1.43	1.34	1.44	1.41	1.40
Trimethylbenzene	4.30	6.74	6.81	7.88	6.28	7.22	5.65	5.86
Ethylmethylbenzene	1.01	1.74	1.50	1.75	1.64	1.54	1.47	2.14
C_{10}	3.35	3.76	3.74	3.92	3.58	3.61	3.77	4.27

correlation with the SiO_2/Al_2O_3 ratio, although there is a slight reverse tendency compared to the former. The increased aromatic compound reduced the olefin content, which means that the olefins formed by the cracking process are aromatics. The content of the olefins and the aromatics are also presented as a function of the mesopore volume of the representative 3.8 nm in Fig. 7. The amount of the mesopore volume increased the aromatics. Also, the result clearly supports that olefins play an important role in aromatic formation during the cracking of VGO on the treated mordenites. Accordingly, aromatics are formed by the cyclization of olefins in the gasoline range. The fraction of aromatics increased with the mesopore volume of 3.8 nm in treated mordenites. This result implies that aromatic products are likely to be diffusion-limited within the two-dimensional structure of pure mordenite. The formation of mesopores converts the mordenite to a more three-dimensional structure and improves the mobility of large molecules by shortening the diffusion path and thus improves the rate of formation of the aromatic compounds.

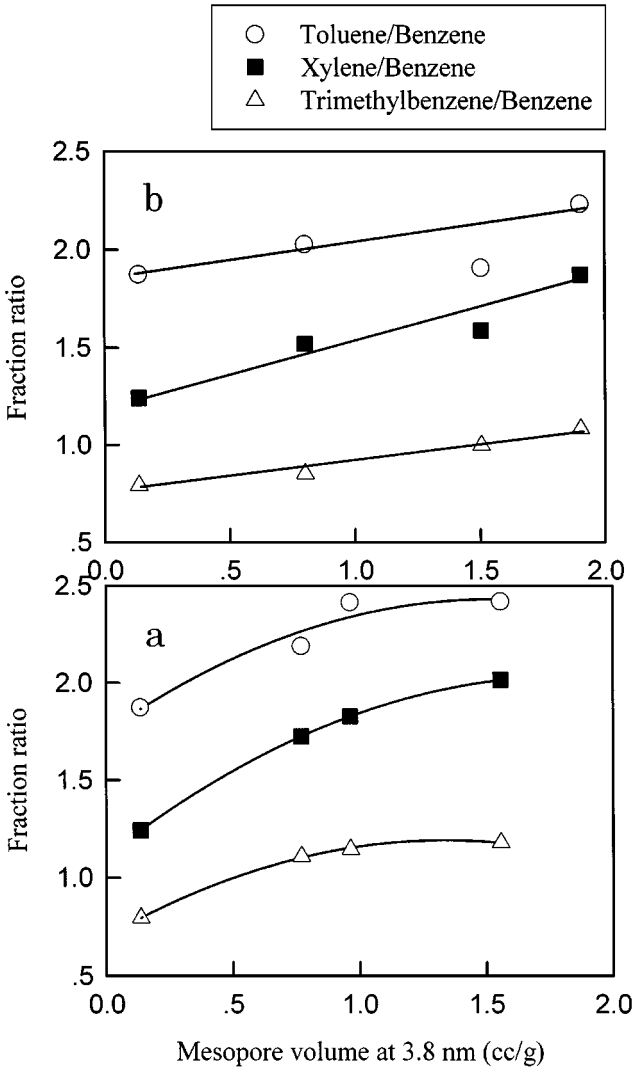

FIG. 8. Fraction ratio of toluene, xylene, and trimethylbenzene to benzene in aromatics as a function of mesopore volume over mordenites treated by either steam/HCl (a) or HF (b).

The fraction ratios of toluene, xylene, and trimethylbenzene to benzene as a function of a mesopore volume of about 3.8 nm in treated mordenites are shown in Fig. 8a and Fig. 8b. They show that the content of the toluene, xylene, and trimethylbenzene increased with the mesopore volume of 3.8 nm. It implies that the fraction of alkylaromatics with methyl groups is strongly influenced by the mesopore volume in treated mordenites. It is interesting to note that no matter what treatment is used in dealumination of mordenites, all the catalysts show the order of the fraction ratio as follows: toluene/benzene > xylene/benzene > trimethylbenzene/benzene. A similar result has been reported that xylene and toluene are obtained as the highest components among aromatics in Y-type zeolites and mordenites, respectively (23, 27). It is concluded that the formation of higher branched aromatics is retarded due to the diffusion limitation and/or to the hindrance of transition state formation.

CONCLUSIONS

Cracking reaction of vacuum gas oil was carried out on two series of mordenites which have a secondary mesopore formed by the treatment of steam/HCl and HF. The mesopore volume increased with the degree of the dealumination, while the micropore volume decreased proportionately. The plots of the conversion of VGO, yield of gasoline and of kerosene + diesel against the acid-amount/mesopore-volume gave a maximum value which is explained as an optimum point of the two opposing tendencies. The one is the decreasing tendency in activity due to reduction of the acid site and the other is the increasing tendency in activity due to mesopore formation with the SiO_2/Al_2O_3 ratio. The treated mordenite of low acid site density and large mesopores shows a higher yield of aromatics in the gasoline fraction. Aromatic compounds were produced by cyclization of olefins formed in the cracking process, and the cyclization can easily occur in the mesopores of treated mordenites. In branched aromatics, toluene is the largest component because the formation of higher branched aromatics is retarded due to diffusion limitation and/or to the hindrance of transition state formation.

ACKNOWLEDGMENT

The financial support of this work by the Research Center for Catalytic Technology (Pohang University of Science and Technology) is gratefully acknowledged.

REFERENCES

1. Corma, A., Martinez, A., Martinez-Soria, V., and Monton, J. V., *J. Catal.* **153**, 25 (1995).
2. Ino, T., and Al-Khattaf, S., *Appl. Catal.* **142**, 5 (1996).
3. Corma, A., and Martinez-Triguero, J., *Appl. Catal.* **118**, 153 (1994).
4. Biswas, J., and Maxwell, I. E., *Appl. Catal.* **58**, 19 (1990).
5. Abbot, J., and Guerzoni, F. N., *Appl. Catal.* **85**, 173 (1992).
6. Choudhary, V. R., and Akolekar, D. B., *J. Catal.* **125**, 143 (1990).
7. Corma, A., Miguel, P. J., Orchilles, A. V., and Koermer, G., *J. Catal.* **145**, 181 (1994).
8. Corma, A., Martinez, A., and Martinez, C., *Appl. Catal.* **134**, 169 (1996).
9. Corma, A., Miguel, P. J., and Orchilles, A. V., *J. Catal.* **145**, 58 (1994).
10. Abbot, J., and Wojciechowski, B. W., *J. Catal.* **115**, 521 (1989).
11. Scherzer, J., *Appl. Catal.* **75**, 1 (1991).
12. "Advances in Fluid Catalytic Cracking," Catalytic Study 4186CC, 1987.
13. Corma, A., Miguel, P. J., and Orchilles, A. V., *Appl. Catal.* **138**, 57 (1996).
14. Horikoshi, H., Kasahara, S., Fukushima, T., Itabashi, K., Okada, T., Terasaki, O., and Watanabe, D., *Chem. Soc. Japan* **3**, 398 (1989).
15. Mauge, F., Courcelle, J. C., Engelhard, Ph., Gallezot, P., and Grosmangin, J., *in* "New Developments in Zeolite Science and Technology" (Y. Murikami *et al.*, Eds.), p. 803. Elsevier, Amsterdam, 1986.

16. Gallezot, P., Feron, B., Bourgogne, M., and Engelhard, Ph., *in* "Zeolites: Facts, Figures, Future" (P. A. Jacobs *et al*., Eds.), p. 128. Elsevier, Amsterdam, 1989.
17. Addison, S. W., Cartlidge, S., Harding, D. A., and Mcelhiney, G., *Appl. Catal.* **45**, 307 (1988).
18. Lee, K. H., and Ha, B. H., *HWAHAK KONGHAK* **34**(3), 363 (1996).
19. Rajagopalan, K., Peters, A. W., and Edwards, G. C., *Appl. Catal.* **23**, 69 (1986).
20. Corma, A., Grande, M., and Fornes, V., *Appl. Catal.* **66**, 45 (1990).
21. Ghosh, A. K., and Kydd, R. A., *J. Catal.* **103**, 399 (1987).
22. Lok, B. M., Gortsema, F. P., Messina, C. A., Rastelli, H., and Izod, T. P., *J. Am. Chem. Soc. Div. Pertrochem. Prepr.* **27**, 470 (1982).
23. Lee, K. H., Ph.D disseration, Hanyang University, Seoul, Korea, 1996.
24. Guisnet, M., and Magnoux, P., *Appl. Catal.* **54**, 1 (1989).
25. *In* "Fluid Catalytic Cracking Process Technology, Section 1, Pittsburgh, PA, September 1992," p. 7.
26. Corma, A., Faraldos, M., Martinez, A., and Mifsud, A., *J. Catal.* **122**, 230 (1990).
27. Lee, K. H., Lee, Y. W., and Ha, B. H., *Ind. Eng. Chem. Res.* **37**(5), 1761 (1998).